JOINT INSTITUTE FOR NUCLEAR RESEARCH

FINAL REPORT ON THE INTEREST PROGRAMME

Radiation Protection and the Safety of Radiation Sources

Participant: Abdelrahman Barakat

Supervisor: Dr. Said Abou El-Azm

Wave 10 (26 February – 14 April, 2024)

Abstract

The implementation of radiation protection measures has been prompted by the growth of activities involving ionizing radiation. This initiative aims to reduce radiation doses, minimize the adverse effects of ionizing radiation, raise awareness of radiation hazards, and prevent unsafe practices, thereby establishing the basis for radiation protection regulations and protocols. the report discusses methods of protection using various detectors, methods of calibration them, and tracking radiation through them.

The tasks were successfully accomplished using various software tools, including ROOT, Excel, and SRIM simulation, based on experimental data obtained in the JINR laboratory.

The technical data of the BGO and NaI detectors were compared, and unknown sources were identified using the calibration line equation with known energy. Additionally, the attenuation coefficients of aluminum and copper, as well as the range of alpha particles in air, were determined and knowing how Pixel detector works and its importance.

Table of contents

List of Figures

List of Tables

BGO Detector

Overview of the detector

A Bismuth Germinate (BGO) detector is a type of scintillation detector that employs a high Z (atomic number) and high-density scintillation material, Bi4Ge3O12. This material is highly effective at absorbing gamma rays, making it ideal for detecting high-energy radiation like gamma rays and X-rays. Moreover, it is mechanically robust, sturdy, and non-hygroscopic, facilitating easy cutting and polishing using established techniques. The high effective atomic number (Z) of BGO enhances the likelihood of a photoelectric event at the initial interaction, thereby reducing inter-crystal scatter and improving detection efficiency.

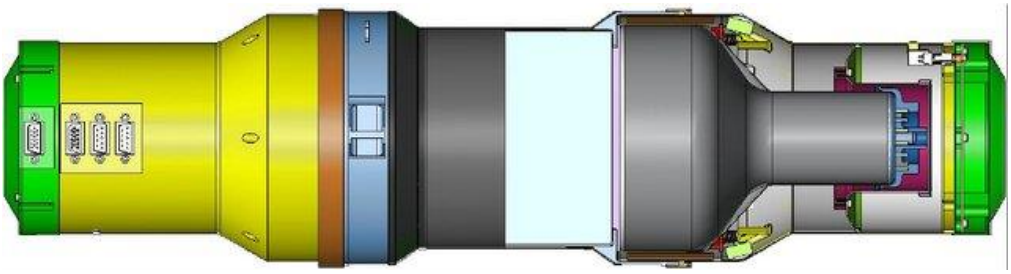

Figure 1: Side-view of the BGO detector unit.

BGO detectors are widely used in various fields, including radiation detection, medical imaging, radio pharmaceuticals, security surveillance, and geographic surveying. They are also utilized in positron emission tomography (PET) detectors.

Resolution

Fitting graphs for different applied voltages and get the Main and Sigma of peaks then, evaluate Resolution according to equation:

$$Reslution = \frac{Sigma}{Mean} * 2.35$$

Table 1: Fitting Results

	CO-60		
Applied Voltage (V)	Mean	Sigma	Resolution
1200	1.41221	0.6088677	1.013191
1300	1.37941	0.269192	0.4586
1400	1.92558	0.274946	0.335547
1500	2.98086	0.434947	0.3428962
1600	4.41538	0.584355	0.31101156
1700	6.12298	0.735375	0.282236
1900	10.7078	1.24092	0.2723399
2000	13.6794	1.58086	0.27157777

According to results of fitting the graphs, get the resolution curve for Co-60 peaks depends on applied volt as shown in Figure:

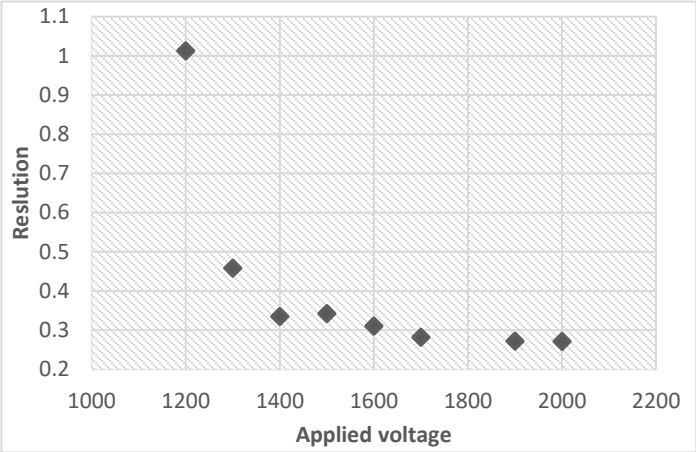

Figure 2: The relation between the Resolution and Applied Volt for BGO detector

Energy Calibration

Calibrate the detector is necessary to ensure that the device is valid or not and that it performs its functions.

- It is noticeable that **BGO** detector can't separate between to peaks of Co-60 which refer to low resolution.

Table 2: Calibration Results

	Energy (Mev)	Mean
Peak 1	0.662	6.48277
Peak 2	1.25	12.251
Peak 3	2.5	24.3523

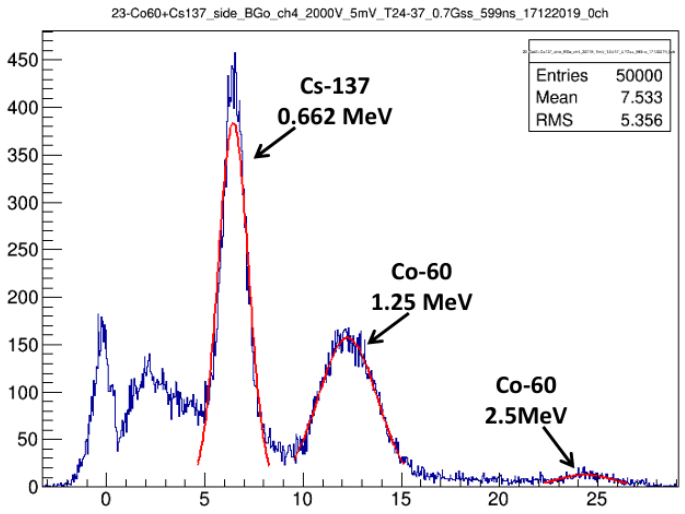

Figure 3: Cs-137 and Co-60 spectrum from BGO detector with 2000V

- By fitting known peaks plotting of energy vs. channel number (mean), get a calibration curve, and the calibration function as shown:

$$Mean = 9.7158 * Energy + 0.0733$$

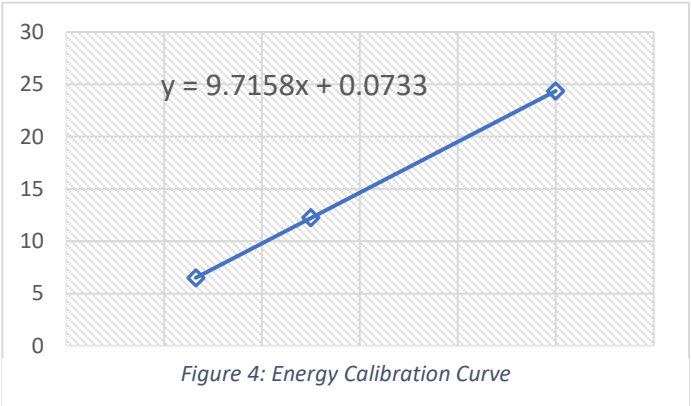

Figure 4: Energy Calibration Curve

Identification of Unknown Sources

Fitting five unknown peaks and get the Mean, then substitute in calibration function to get the Energy of unknown element and finally compare between energies table.

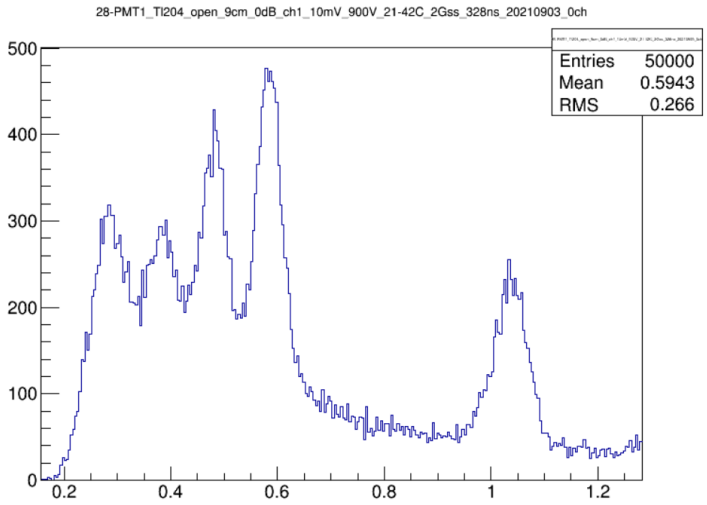

Figure 5: Unknown spectrum by BGO detector

Table 3:Identify unknown sources using calibration function

Calculating the energy of every peak using calibration curve				
	Mean	Sub in Calibration Function	x (Energy for unknown element) (Mev)	Expected Element
Peak 1	0.289602	0.289602 = 9.7158x + 0.0733	0.0222629	Sm-151
Peak 2	0.381457	0.381457 = 9.7158x + 0.0733	0.03171709	Mg-28
Peak 3	0.47737	0.47737 = 9.7158x + 0.0733	0.04158895	Rh-103m (OR) I-129
Peak 4	0.583767	0.583767 = 9.7158x + 0.0733	0.52539883	Te-132
Peak 5	1.03504	1.03504 = 9.7158x + 0.0733	0.09898721	Gd-153 (OR) Au-195

NaI Detector

Overview of the detector

A NaI detector, a scintillation detector, employs a sodium iodide crystal doped with thallium NaI to detect ionizing radiation, specifically gamma rays and X-rays. Upon radiation exposure, the NaI crystal emits short light pulses, which are then transformed into electrical signals by a photomultiplier tube (PMT) attached to the device. These electrical signals vary in proportion to the radiation's energy, enabling the analysis of the radiation's energy spectra.

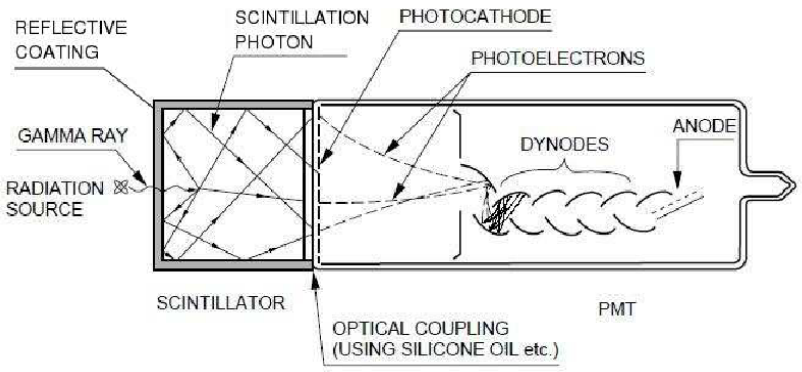

Figure 6: Photomultipliers Tubes (PMT)

NaI detectors find widespread use in radiation detection, medical imaging, radio pharmaceuticals, security surveillance, and geographical surveys due to their high light output, rapid decay time, and cost-effectiveness, making them a favored option for various radiation detection applications

Resolution

By fitting spectrum graph and get the main and sigma of peaks, evaluate Resolution according to equation:

$$Reslution = \frac{Sigma}{Mean} * 2.35$$

Table 4: Fitting Results

	CO-60					
Applied Voltage (V)	Mean		Sigma		Resolution	
	Peak 1	Peak 2	Peak 1	Peak 2	Peak 1	Peak 2
900	23.66	26.566	0.618712	0.608548	0.061453	0.0538315
1000	40.6401	45.4568	0.98599	0.999523	0.0570145	0.0516727
1100	65.7819	73.2779	1.52299	1.50844	0.0544075	0.0483752
1200	98.7506	108.512	2.00217	1.87064	0.047646	0.040511
1300	137.357	148.84	2.59941	2.4422	0.0444725	0.0385593

According to results of fitting the graphs, get the two resolution curves for Co-60 peaks depends on applied volt as shown in Figure:

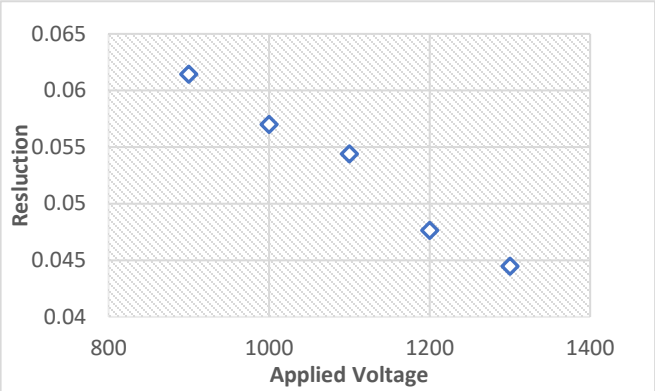

Figure 8: Peak1 Resolution, relation between the Resolution and Applied Volt

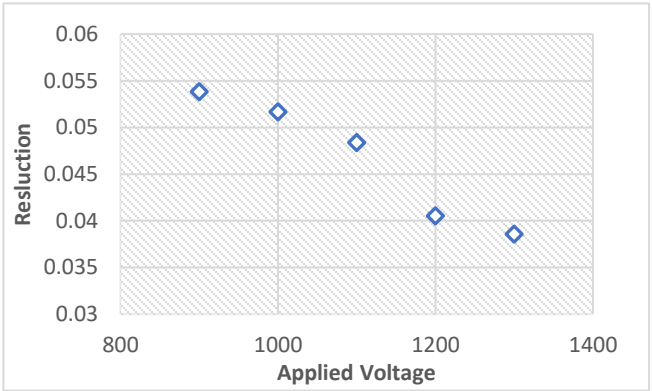

Figure 7:Peak2 Resolution, relation between the Resolution and Applied Volt

Energy Calibration

According to results of fitting the graph, get the resolution curve for two Co-60 peaks depends on applied volt:

- It is noticeable that **NaI** detector has better resolution than **BGO** detector that can separate two Co-60 peaks

Table 5: Calibration Results

	Energy (Mev)	Mean
Peak 1, Cs-137	0.662	7.70283
Peak 2, Co-60	1.173	12.6219
Peak 3, Co-60	1.332	14.1436
Peak 4, Co-60	2.5	25.1889

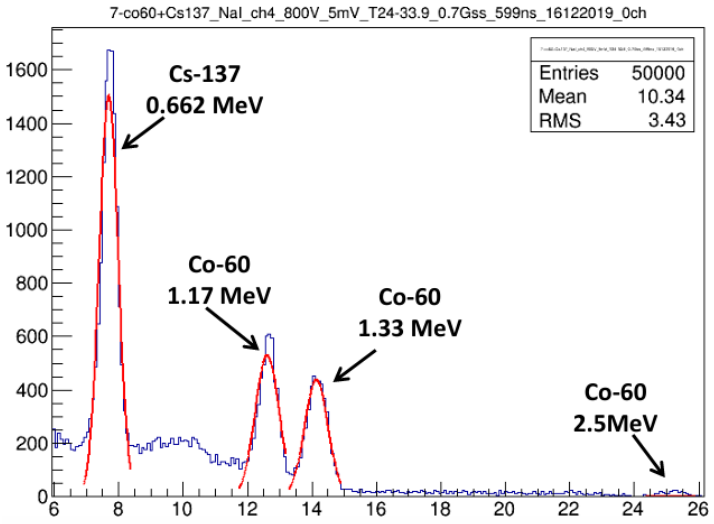

Figure 9: Cs-137 and Co-60 spectrum from BGO detector with 800V

- By fitting known peaks plotting of energy vs. channel number (mean), get a calibration curve, and the calibration function as shown:

$$Mean = 9.6163 * Energy + 1.3378$$

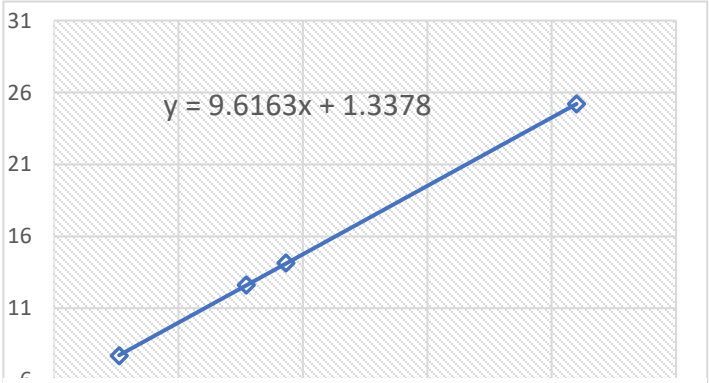

Figure 10: Energy Calibration Curve

Identification of Unknown Sources

Fitting four unknown peaks and get the Mean, then substitute in calibration function to get the Energy of unknown element and finally compare between energies table.

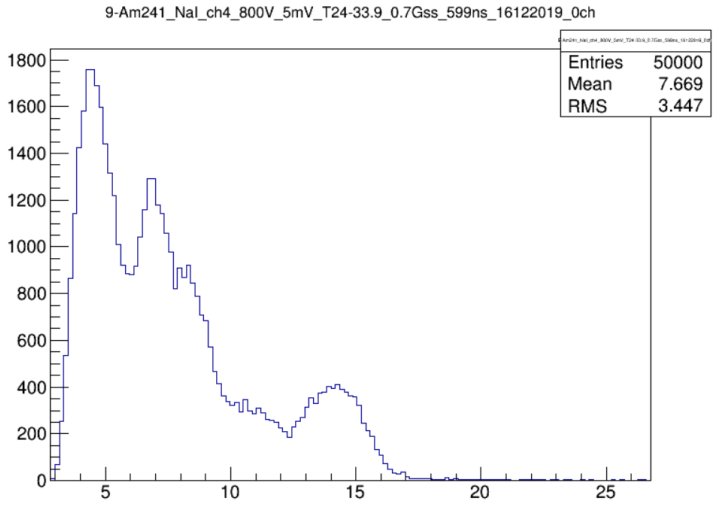

Figure 11: Unknown spectrum by NaI detector

Table 6: Identify unknown sources using calibration function

Calculating the energy of every peak using calibration curve				
	Mean	Sub in Calibration Function	x (Energy for unknown element) (Mev)	Expected Element
Peak 1	4.64213	4.64213 = 9.6163x + 1.3378	0.343617	Eu-152 or Ag-111
Peak 2	6.89746	6.89746 = 9.6163x + 1.3378	0.5781496	Tl-208
Peak 3	8.1696	8.1696 = 9.6163x + 1.3378	0.71043956	Te-129m or Zr-95
Peak 4	14.0109	14.0109 = 9.6163x + 1.3378	1.317877	Ca-47 or Co-60

Alpha Particle (α) Range in Air

Objective

Range defined as a distance alpha particle travel through the medium before losing its energy and get absorbed, due to positive charge, α particles have great ionizing power, but their large mass results in very little penetration. According to Energy of alpha particle can travel a few centimeters, and their penetration through other material is negligible.

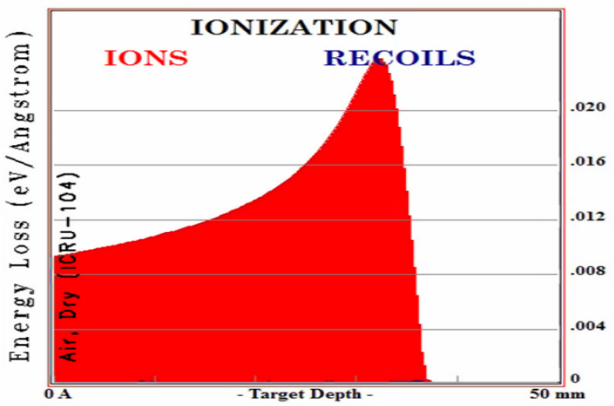

Figure 12: Bragg curve of alpha particles in 5 cm air.

Results

According to the experiment's data analysis, the table and plot reveal a decrease in counts per second as the distance increases, eventually stabilizing at a constant level, indicating no further signal detection. This suggests that the range of alpha particles in air is approximately 3.5 cm.

Table 7: Number of counts/second of source at different distances from the detector.

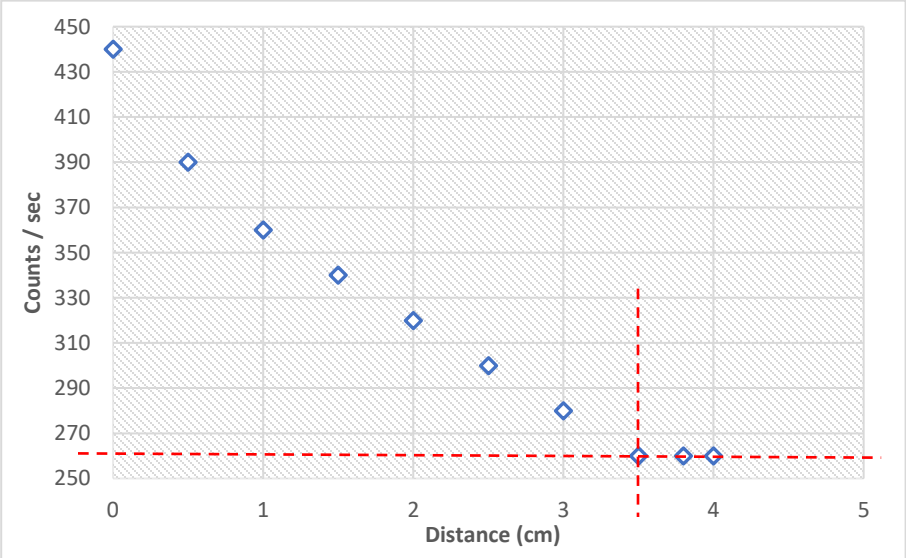

Figure 13: The range of alpha particles in air

Source Pu239, Energy 5.5 (MeV)	
Detector: Plastic	
Applied volt: 2000V	
Distance, cm	Counts/Sec
0	440
0.5	390
1	360
1.5	340
2	320
2.5	300
3	280
3.5	260
3.8	260
4	260

∴ R =3.5 cm

Attenuation Factor (μ)

Objective

Measure attenuation curves of gamma radiation with various photon energies, using various absorbers.

The basic property of the absorption of gamma rays is the exponential decrease in the intensity of radiation as a homogenous beam of gamma rays passes through a thin slab of matter. When a beam of gamma rays of intensity $\boldsymbol{I}$ is incident on a slab of thickness $\boldsymbol{dx}$, the change in intensity of the beam as it passes through the slap is proportional to the thickness and to the incident intensity:

$$d(I) = -\mu\, I\, d(x)$$

where the proportionality constant μ is called the attenuation (absorption) coefficient, The μ depends on the nature of the absorber and on the initial energy of gamma rays, by integrating the previous equation:

$$I = I_0\, exp(-x\mu)$$

- $\boldsymbol{I}$: incident on a slab of thickness
- $\boldsymbol{I_0}$: is an intensity at no matter
- $\boldsymbol{x}$: thickness of matter
- μ : Attenuation coefficient

Results

According to the results by using two different materials thicknesses (Copper & Aluminum), get two attenuation graphs as shown in Figures

1. Aluminum:
   From the non-linear fitting curve, the obtained linear attenuation coefficient of aluminum (Al) is: $0.439 \pm 0.01725\ cm^{-1}$.
   Comment:
   Compared to real attenuation coefficient of Aluminum, there is a big error in measurement

Table 8: Al thickness to reduce the intensity

Al	
Thickness, cm	I/I0
0	1
0.15	0.75573
0.3	0.71623
0.45	0.70569
0.75	0.68596
0.9	0.67155
1.08	0.66103
1.26	0.63939
μ = 0.439	

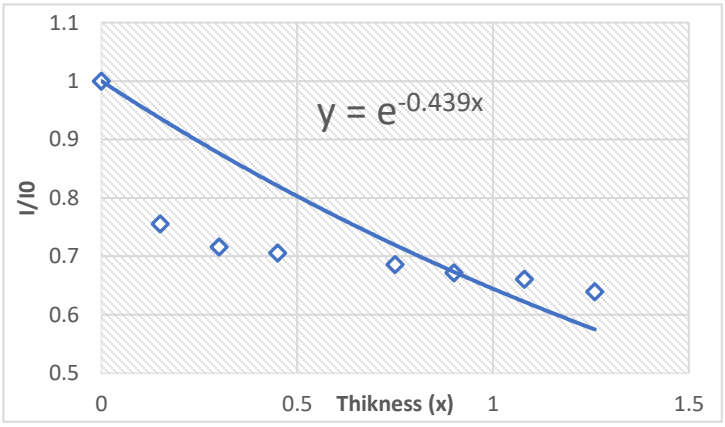

Figure 14: Determination of attenuation coefficient for Al

2. Copper

   From the non-linear fitting curve, the obtained linear attenuation coefficient of copper (Cu) is: $0.663 \pm 0.0471\ cm^{-1}$.

Table 9: Cu thickness to reduce the intensity

Cu	
Thickness, cm	I/I0
0	1
0.2	0.73931
0.25	0.7357
0.4	0.68065
0.8	0.58611
1	0.53827
1.2	0.48042
μ = 0.663	

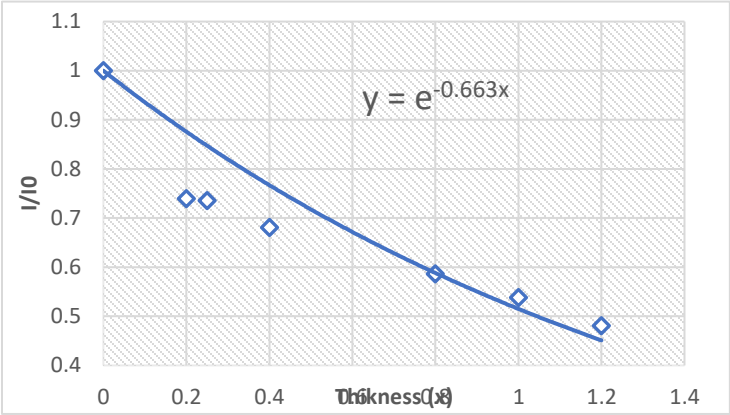

Figure 15: Determination of attenuation coefficient for Cu

Pixel Detector (PD)

Overview of the detector

Hybrid pixel detectors represent a category of ionizing radiation sensors comprising an array of diodes constructed using semiconductor technology alongside their associated electronics. The term "hybrid" originates from the independent manufacturing of the two primary components of these devices, namely the semiconductor sensor and the readout chip - referred to as an application-specific integrated circuit or ASIC-, which are subsequently interconnected through a bump-bonding technique. Ionizing particles are identified as they generate electron-hole pairs upon interacting with the sensor element, typically composed of doped silicon or cadmium telluride. The readout ASIC is divided into pixels that integrate the essential electronics for amplifying and quantifying the electrical signals produced by the incoming particles within the sensor layer.

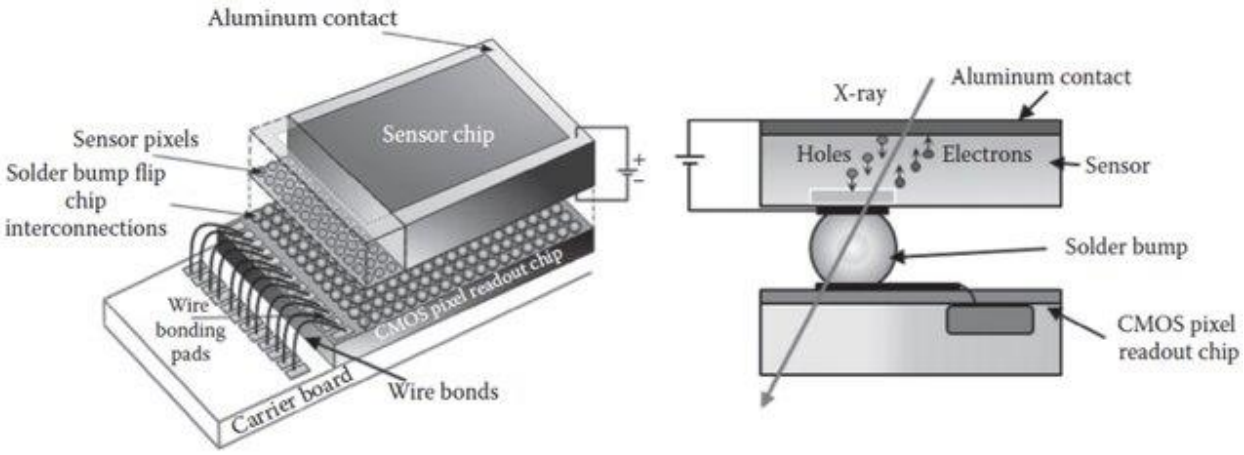

Figure 16: General architecture of a hybrid pixel detector

Determination of alpha range particles in air using pixel detectors:

The determination of alpha range particles in air using pixel detectors involves the measurement of the distance traveled by alpha particles in air before they lose all of their energy. This is important for understanding the behavior and impact of alpha particles in various applications, such as radiation protection and nuclear physics.

The range of alpha particles in air can be determined by measuring the energy of the particles and comparing it to the expected energy loss per unit distance in air by plotting the number of counts per second against the distance traveled by the alpha particles, a curve can be obtained that shows the decrease in energy as the distance increases, The range of alpha particles in air can then be estimated from the point at which the number of counts becomes constant, indicating that the alpha particles have lost all of their energy.

Pixel detectors offer several advantages for the determination of alpha range particles in air. They can measure the energy and position of individual alpha particles with high precision, allowing for accurate determination of the range and energy distribution of the particles. Additionally, pixel detectors can be operated in different modes, such as time-over-threshold mode, which allows for the measurement of the energy deposited in each pixel, providing additional information about the alpha particles.

Determination the range of α-particles with (Am-241) energy about 4 MeV in air using pixel detector

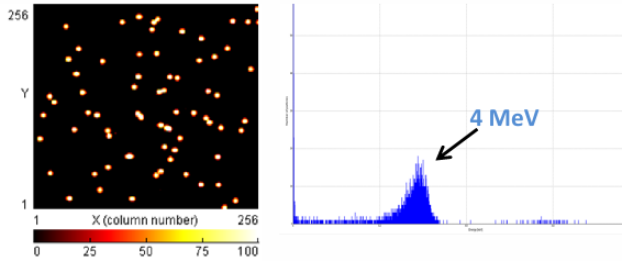

Figure 20: Absorption of alpha particle energy in the air at 0 cm

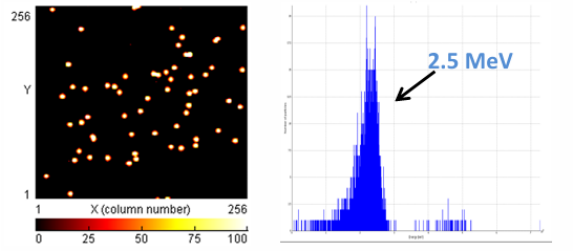

Figure 17: Absorption of alpha particle energy in the air at 1 cm

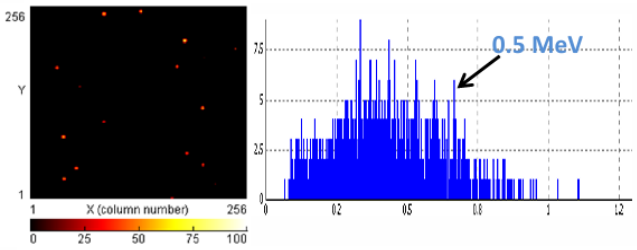

Figure 18: Absorption of alpha particle energy in the air at 2 cm

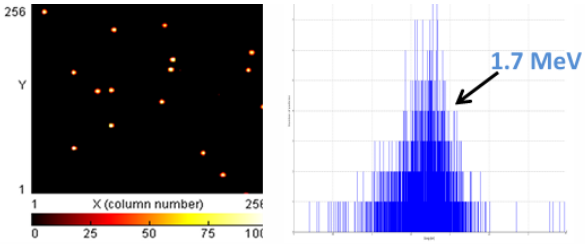

Figure 19: Absorption of alpha particle energy in the air at 2.5 cm

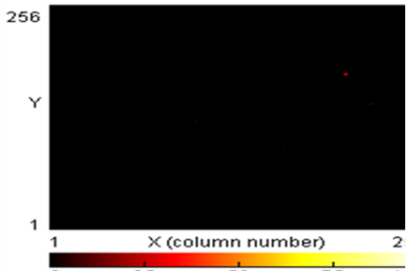

Figure 21: Absorption of alpha particle energy in the air at 3 cm

Conclusion

Throughout this course, the primary objective has been to equip by essential knowledge required for effective radiation protection and the management of diverse radiation sources. A key focus has been on the comprehensive study of various scintillation detectors, delving into the intricacies of their operation and calibration processes to ensure their accuracy and functionality. By understanding how to calibrate detectors effectively, having the necessary skills to validate detector performance and reliability.

An integral aspect of this course has been the exploration of identifying unknown radiation sources through calibration functions, a critical skill in radiation detection and analysis. By utilizing advanced software tools like ROOT, SRIM simulation, and Excel, participants have been able to analyze and interpret data effectively, enhancing their understanding of radiation detection mechanisms and processes.

Furthermore, the course has facilitated a detailed comparison between the resolution capabilities of BGO and NaI detectors, shedding light on their respective strengths and limitations in radiation detection applications. By verifying unknown sources using each detector, participants have honed their practical skills in radiation source identification and analysis.

The determination of attenuation coefficients for aluminum and copper using a Plastic detector at 2000 V with Cs-137 as the radioactive source has been a significant component of this course. Understanding attenuation, the reduction of an x-ray beam as it passes through different materials, and the unique attenuation coefficients associated with each material are crucial for effective radiation shielding and safety measures.

Lastly, the course has emphasized the characteristics of alpha particles, highlighted their heavy charged nature and limited penetrating power. With an average range of approximately 3.5 cm in air, alpha particles exhibit short-travel distances due to their high charge and mass, a fundamental concept in radiation physics and protection strategies.

Acknowledgements

The program was completed fully thanks to the periodic follow-up from JINR INTEREST Program, and good cooperation from the supervisor, Dr. Said Abou El-Azm.